Journal of Materials Chemistry A

Accepted Manuscript

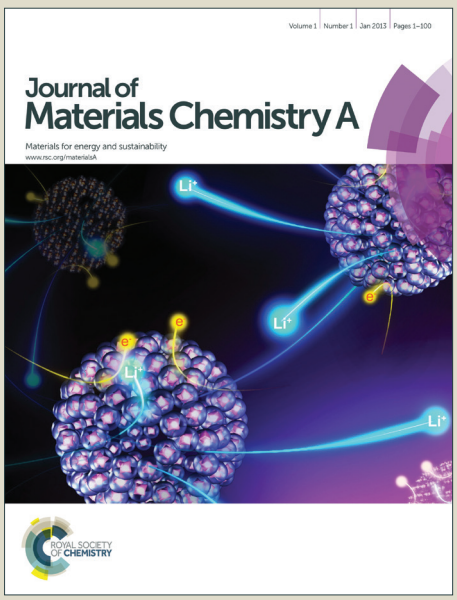

ROYAL SOCIETY OF CHEMISTRY

www.rsc.org/materialsA

Journal Name

RSCPublishing

ARTICLE

AuPd bimetallic nanoparticles decorated on graphene nanosheets: their green synthesis, growth mechanism and high catalytic ability in 4-nitrophenol reduction

Xiaomei Chen,* [a, c] Zhixiong Cai, [b] Xi Chen* [b] and Munetaka Oyama [c]

Cite this: DOI: 10.1039/xoxxoooooox

Received ooth January 2012,
Accepted ooth January 2012

DOI: 10.1039/xoxxoooooox

www.rsc.org/

A one-pot green method to synthesize ultrafine AuPd nanoparticles (NPs) monodispersed on graphene nanosheets (GNs) is reported. Due to the reducing capability, moderate number of depositing sites and large surface area, GNs is used as a three-functional agent such as reductant, stabilizer and support in this synthesis. The morphology, structure and composition of thus-prepared AuPdNPs/GNs were characterized by transmission electron microscopy (TEM), high resolution TEM, energy-dispersive X-ray spectroscopy and X-ray photoelectron spectroscopy. As it is a surfactant-free formation process, the as-prepared AuPdNPs/GNs is very clean and can exhibit a high activity towards the reduction of 4-nitrophenol. Moreover, the optical properties and catalytic activities of the AuPdNPs/GNs composite are tunable via the Au versus Pd atomic ratio as controlled in their synthesis. The catalytic activity of bimetallic AuPdNPs/GNs composites is highly enhanced over the monometallic AuNPs/GNs and PdNPs/GNs composite. This straightforward method is of significance for deposition bimetallic NPs with high catalytic performance on graphene-based materials.

Introduction

Bimetallic nanoparticles (NPs) have been attracting growing attentions owing to their composition-dependent optical, electronic, and catalytic properties, which lead to a wide range of applications.[1-4] Heterogeneous catalysis is one of the most important applications of bimetallic NPs.[5-9] As the catalytic reactions take place only on the surface of the NPs, slight changes in the structures, sizes, or chemical compositions of bimetallic NPs can influence their catalytic properties.[10-13] It has been realized that NPs with ultrafine size can increase the surface area, the number of edges and corner atoms, which greatly improve their catalytic properties.[14-17] Therefore, it is interesting to produce bimetallic NPs as small as possible to increase the accessible surface atoms. However, as the particle size is reduced, the surface energy of NPs increases, which make the NPs unstable with promoting for inter-particle aggregations. To avoid the aggregation, various stabilizers such as polymers,[18] dendrimers,[19] metal organic frameworks,[20] as well as different types of ligands[21] have been used as capping agents to stabilize NPs. However, the presence of capping agents around the NPs may severely limit their chemical activities.

As we mentioned above, it is fairly difficult to obtain ultrafine NPs especially in the absence of a stabilizer. On the other hand, in view of new and important commercial opportunities, it is important to meet the green chemistry principles for the overall procedure of the preparation of NPs, to minimize reactant consumption and by-product production, and to use, if possible, renewable materials and benign solvents. Therefore, it is of great importance to find out a green and efficient method to prepare NPs with high catalytic ability.

Recently, we have found that PdNPs can grow directly on graphene oxides (GO) through a spontaneous redox reaction.[22] As it is a surfactant-free formation process, the as-prepared catalyst is very "clean" and can exhibit high electrocatalytic ability. This provides a hint that the special 2D structure of graphene-based materials may limit the migration and aggregation of metal NPs. So far, there are many reports about fabrication bimetallic NPs loaded on graphene nanosheets (GNs), but only few of them through surfactant-free processes.[23-25] Anandan et al. demonstrated a sonochemical method for the formation of GNs supported PtSn catalysts by the co-reduction of GO, $SnCl_2$ and H_2PtCl_6 using ethylene glycol.[23] More recently, Qian et al. developed a solvothermal process to deposit PtPdNPs and PtCoNPs on exfoliated GNs by the reduction of ethanol.[24] In these synthesis, special instruments such as autoclave or sonifier are necessary and the reactions usually operated under high temperature and take a long time. To the best of our knowledge, no attempt has been

made to use GNs to reduce bimetallic precursors directly with restricting the size of bimetallic NPs.

In the present paper, we demonstrate ultrafine and well-dispersive AuPdNPs can be produced on GNs by facile mixing bimetallic precursors and GNs in aqueous solution at room temperature. Different from previous studies, the reaction is so quickly that only 5 min is enough for our synthesis. And more importantly, no reductant or surfactant was necessary in this synthesis. Due to the high-density, ultrafine, monodisperse and pristine properties of AuPdNPs, the AuPdNPs loaded GNs (AuPdNPs/GNs) reveal a high activity for the reduction of 4-nitrophenol (4-NP). Moreover, taking the advantage of synergetic effect between Au and Pd, the obtained catalyst exhibits superior activity compared with monometallic AuNPs/GNs and PdNPs/GNs.

Experimental

Materials

K_2PdCl_4 and $NaBH_4$ were purchased from Wako Pure Chemicals, Co. Ltd. (Japan); graphite powder, $HAuCl_4$, 4-nitrophenol and hydrazine were from Aldrich Chem Co. (USA). All other reagents were of analytical grade and used without further purification. The pure water for solution preparation was from a Millipore Autopure WR600A system (USA).

Instrumentations

Morphologies and crystal structures of AuPdNPs/GNs observed by transmission electron microscopy (TEM) and high-resolution TEM (HRTEM) were performed on a TECNAI F-30 TEM with an acceleration voltage of 300 kV. Energy dispersive X-ray spectroscopy (EDX) analysis, high-angle annular dark-field scanning TEM (HAADF-STEM), and inductively coupled plasma mass spectrometry (ICP-MS) were used to identify the elemental composition of the complex. All TEM samples were prepared by depositing a drop of diluted suspension in water on a copper grid coated with carbon film. Electronic binding energies of AuPdNPs/GNs were measured by X-ray photoelectron spectroscopy (XPS) analysis which was performed on a PHI Quantum 2000 Scanning ESCA Microprobe with a monochromatised microfocused Al X-ray source. All the binding energies were calibrated by C1s as reference energy (C1s = 284.6 eV). The phases of the as-prepared products were determined by means of the powder X-ray diffraction (XRD) pattern, recorded on a Panalytical X-pert diffractometer with Cu Kα radiation. The ultraviolet-visible (UV-vis) absorption spectra of catalysts for the reduction of 4-NP were measured on a UV 1240V spectrometer (Shimadzu, Japan).

Preparation procedures

Synthesis of GO and GNs. GO and GNs were prepared according to a modified Hummer's method[26]. 50 mg as-synthesized product was dispersed in 100 mL water to obtain a yellow-brown aqueous GO solution (0.05 wt%) with the aid of ultra-sonication. GNs were synthesized following Li's method[27]: 50 mL as-prepared GO solution was mixed with 50 mL water, 50 μL hydrazine solution (35 wt% in water) and 350 μL ammonia solution (25 wt% in water) in a 250 mL glass vial. After being vigorously stirred for 5 min, the vial was put in an oil bath (95 ^oC) for 1 h. Finally, the obtained GNs colloids were set aside for one month to remove the residual hydrazine.

Synthesis of catalysts. In a typical synthesis of AuPdNPs/GNs, homogeneous GNs colloids (5 mL 0.025 wt%) and $HAuCl_4$ (0.5 mL 10 mM) aqueous solution was kept in a glass bottle under vigorous stirring for 1 min, and then K_2PdCl_4 (0.5 mL 10 mM) aqueous solution was added and kept stirring for another 4 min at room temperature. Then, the reaction mixture was washed with pure water and centrifuged to remove the remaining reagents. For comparison, other catalysts were also prepared using the same method; the starting materials were (1) homogeneous GNs colloids (5 mL 0.025 wt%) and K_2PdCl_4 (0.5 mL 10 mM) aqueous solution for PdNPs/GNs, (2) homogeneous GNs colloids (5 mL 0.025 wt%) and $HAuCl_4$ (0.5 mL 10 mM) aqueous solution for AuNPs/GNs, (3) homogeneous GNs colloids (5 mL 0.025 wt%) and aqueous solutions of 0.5 mL 10 mM $HAuCl_4$ and v mL 10 mM K_2PdCl_4 (v=0.125, 0.25, 0.75, 1.0) for Au_xPd_yNPs/GNs.

Catalysis procedures

The reduction of 4-NP by $NaBH_4$ was chosen as a model reaction to test the catalytic activity of the catalysts. Typically, the reaction was carried out in a quartz cuvette with an optical path length of 1 cm and monitored using UV-vis spectroscopy at 25 °C. 1 mL of aqueous 4-NP solution (0.1 mM) was mixed with 1.0 mL of a fresh $NaBH_4$ solution (10 mM), resulting in an immediate color change from light yellow to yellow-green. Immediately after adding 5 μL 0.25 mg mL^{-1} AuPdNPs/GNs (1.25 μg, 25.2 wt% of Au content), the mixture solution was quickly measured by UV-vis spectroscopy in a scanning range of 250-500 nm. The change of absorption was recorded in situ to obtain the successive information about the reaction. As the reaction proceeded, it could be observed that the solution color changed gradually from yellow to colorless. Following the similar procedures, PdNPs/GNs, AuNPs/GNs and Au_xPd_yNPs/GNs (each for 1.25 μg) were also used as heterogeneous catalysts for the reduction of 4-NP.

In the recycle test, four recycles of the activity were examined for AuPdNPs/GNs. After the first run, 5 μL 20 mM 4-NP and 10 μL 1 M $NaBH_4$ solution were directly added into the reaction mixture for the second run and the same process for the third and fourth run.

Results and discussion

Characterization of AuPdNPs/GNs

In our previous studies, we discovered that ultrafine PdNPs can be well-dispersed on GO surface by the redox reaction between $PdCl_4^{2-}$ and GO.[22] In connection with our previous and ongoing research on spontaneous reduction method to synthesize NPs,

we discovered that AuPdNPs/GNs could be obtained easily by stirring the mixture containing GNs, $AuCl_4^-$ and $PdCl_4^{2-}$ at room temperature for 5 min. Fig. 1 shows the representative TEM images of the as-synthesized AuPdNPs/GNs at different magnifications. It is striking that AuPdNPs are homogeneously dispersed on the surfaces of GNs. Moreover, according to the result of particle size distribution histogram (Fig. S1), the average size of AuPdNPs was 3.46 nm, and the relative standard deviation (RSD) of the NPs' size is 8.1%, suggesting that the monodispersion of these AuPdNPs. A representative HRTEM image of AuPdNPs shows the (111) lattice fringe distance of 0.23 nm (Fig. 1D), which is between the (111) lattice spacing of face-centered cubic (fcc) Au (0.24 nm) and fcc Pd (0.22 nm) NPs.

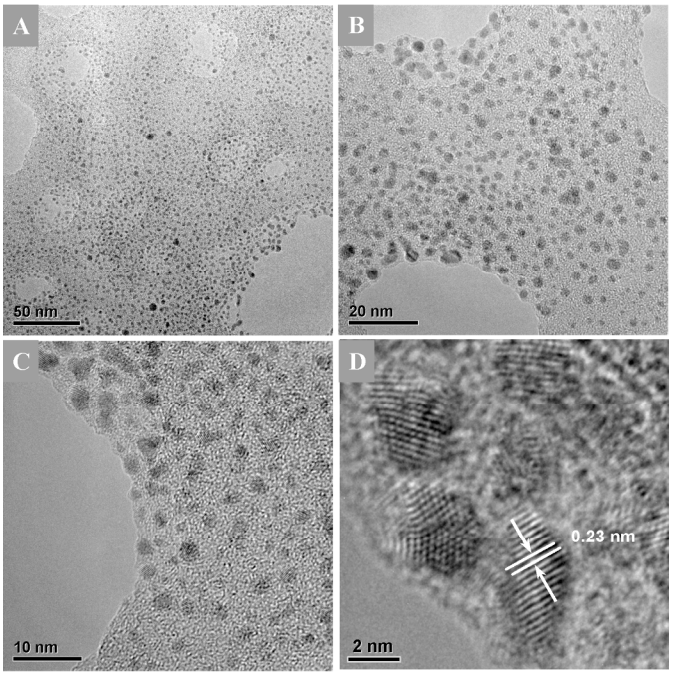

Fig. 1 (A-C) Representative TEM and (D) HRTEM images of as-prepared AuPdNPs/GNs.

To investigate the elemental composition of AuPdNPs, the product was further characterized by HAADF-STEM technique (Fig. 2A-C). Here, it is necessary to mention that for the ultrafine AuPdNPs, it is really difficult to get their HAADF-STEM results. Therefore, AuPdNPs with some aggregations are found for the HAADF-STEM test. According to Fig. 2B and C, it was clearly shown that both Au and Pd had a homogeneous distribution in each NP, suggesting the formation of AuPd alloy. The alloy structure can be further supported by XRD patterns (Fig. 2D). Very weak diffractions were detected for Au and Pd from XRD patterns of as-synthesized catalysts, indicating the formation of small NPs[6]. Furthermore, compared to the (111) diffraction peak of PdNPs/GNs, the diffraction peak of AuPdNPs/GNs shifted to lower 2θ values towards the Au (111) peak because of the increase of the lattice parameters, revealing a high alloyed level of AuPdNPs. Additionally, it should be pointed out that for the ultrafine NPs, only the weak (111) diffraction peak was identifiable, which might cause a big error in calculating the size of NPs by the Scherrer formula (Table S1). XPS results (Fig. 2E-G) show the doublets $3d_{5/2}$ and $3d_{3/2}$ for Pd and $4f_{7/2}$ and $4f_{5/2}$ for Au, respectively. This also indicates the formation of AuPd alloy composition on the surface of NPs. Moreover, compared to the standard Au (0) and Pd (0), these values are slightly shifted to lower binding energies, suggesting the electrons transfer to Au and Pd metal. Due to the large π-π conjugation on GNs, it can be reasonably deduced that these electrons came from GNs, which would be an evidence of the interaction between AuPdNPs and GNs.

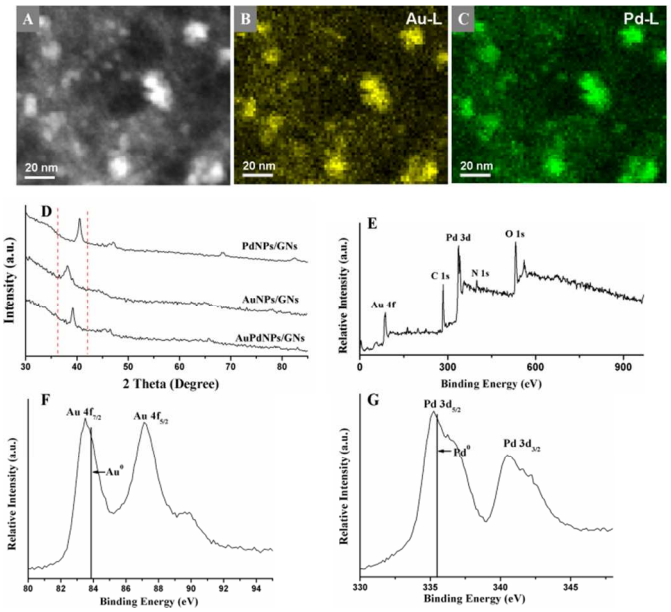

Fig. 2 (A-C) HAADF-STEM characterization of (A) AuPdNPs/GNs and elemental mapping of (B) Au, (C) Pd. (D) XRD patterns of PdNPs/GNs, AuNPs/GNs and AuPdNPs/GNs. (E-G) XPS spectra of (E) AuPdNPs/GNs, (F) Au 4f and (G) Pd 3d.

The ability to prepare ultrafine and monodisperse AuPd alloys directly on GNs is the most striking feature of the proposed synthesis. In a previous paper, it was found that N-induced defects were generated on the GNs after reducing GO with hydrazine, and then Au sub-nanoclusters were nucleated and grown at the defects of GNs. [28] This was supported by the results of first-principles density-functional theory (DFT) calculations.[29] In spite of these reports,[28, 29] it should be mentioned that as hydrazine was used in the preparation of GNs, even the GNs colloids were set aside for one month before reaction with $AuCl_4^-$, it is still important to testify whether the removal of residual hydrazine is complete or not in this synthesis. According to Li's report[27], the weight ratio of hydrazine to GO at 7:10 is a minimal and optimal ratio for producing stable GNs dispersions. Therefore, in our synthesis of GNs, the weight ratio of hydrazine to GO at 7:10 was used. Moreover, they pointed out that the residual hydrazine will cause agglomerations of GNs in a short time. Based on our experiment, the as-synthesis GNs can keep its stable dispersions for more than one year. This can support that all of,

or at least, most of the hydrazine has been consumed in the reduction of GO. To further verify the complete removal of the hydrazine, a test was designed: a small amount of NaCl was added in 10 mL of the fresh prepared GNs colloids to make the aggregations of GNs. Then, the solution was centrifuged and the upper liquid was collected and set aside for one month. After that, 5 mL of the upper liquid was mixed with $HAuCl_4$ (0.5 mL 10 mM) aqueous solution under vigorous stirring for 10 min. No color changed or agglomerations appeared during the reaction. A drop of the solution was deposited on a copper grid coated with carbon film for TEM characterization and no NPs can be observed from the TEM images. This result supported that the removal of residual hydrazine is complete before the introduction of aqueous solution of $HAuCl_4$. Moreover, if the amount of hydrazine was reduced in the synthesis of GNs, the as-synthesized GNs could also react with $AuCl_4^-$ to form AuNPs/GNs, but the density of AuNPs (Fig. S2) is much lower than that observed in Fig. 4A, which may be due to the lower reduction level of GO. This can also support that the AuNPs were formed by the spontaneous redox of $AuCl_4^-$ and GNs, but not the residual hydrazine, and a suitable reducing capability of GNs is important in this synthesis. To investigate the functional group variations on GNs before and after the deposition of AuPdNPs, the deconvoluted XPS spectra of C 1s was studied. As shown in Fig. S3, comparing with GNs, after reaction, the main peak is still at the binding energy of 284.7 eV, which denote to C-C with sp^2 orbital. However, another two peaks at the binding energies of 286.8 and 288.3 eV represented the C-O and C=O functional groups increased, respectively. This indicated that after reduction, oxygenated functional groups were generated on the GNs, however, the amount is very small.

In our synthesis, $AuCl_4^-$ and $PdCl_4^{2-}$ were added stepwisely into the GNs solution. Under some conditions, AuNPs or Au nuclei would be produced first, and then Pd shells might be formed over the Au cores. However, in the present case, AuPdNPs have been formed not as a core/shell structure but as AuPd alloy. This indicates that, in the first step, only small Au nuclei would be produced, and then, in the second step, the co-reduction of $PdCl_4^{2-}$ and remnant $AuCl_4^-$ took place on GNs. In the second step, some Pd nuclei might be formed on GNs because the results of first-principles DFT calculations indicated that Pd could interact with and bind more strongly to GNs compared with Au.[30, 31] However, the co-reduction of $PdCl_4^{2-}$ and $AuCl_4^-$ should be a key step to form the AuPd alloy. Actually, there is a difference in the reduction potentials between Au ($AuCl_4^-$/Au=1.002 V *vs.* the standard hydrogen electrode (SHE))[32] and Pd (Pd^{2+}/Pd = +0.915 V *vs.* SHE)[33], so that the galvanic replacement might happen. As a result, Pd (0) may react with $AuCl_4^-$ to form Au (0) and PdOx. This can be supported that some oxidized species (PdOx) exist in Fig. 2G. To study the reactions in more detail, the deconvoluted XPS spectra of Pd 3d is shown in Fig. S4, in which the relative intensities of the different Pd species are also given. Base on the results, the relative intensity of PdOx was 34 %, which is much lower than that of the native state of Pd, suggesting that the electron transfer reaction between Pd (0) and $AuCl_4^-$ to form Au (0) would not be very significant in the present case. This can also be supported that the sufficient formation of Pd (0) was confirmed in the result of HAADF-STEM (Fig. 2C), and when the reaction time was prolonged from 5 min to 30 min, almost no changes were observed in morphologies or sizes of AuPdNPs (Fig. S5). The latter indicates that the formation of AuPdNPs proceeded in a short time without affected by any further nucleation growth or ripening. Judging from these results, it is considered that GNs prepared by reducing GO with hydrazine not only have moderate reducing capability, the moderate number of depositing sites, but also can offer a strong binding ability to confine and prevent the further growth of NPs, which give rise to the ultrafine and monodisperse properties of AuPdNPs.

Catalytic properties of AuPdNPs/GNs

Inspired by the attractive properties, such as monodisperse, ultrafine, and pristine, of the AuPdNPs on GNs, we explored the catalytic ability of the as-prepared AuPdNPs/GNs. The reduction of 4-NP to 4-aminophenol (4-AP) was carried out as a benchmark reaction using $NaBH_4$ as the reducing agent and AuPdNPs/GNs as the catalyst. It is well-known that the reaction does not proceed without any catalysts because the kinetic barrier between the mutually repelling negative ions 4-NP and BH_4^- is very high. However, in the presence of AuPdNPs/GNs, the composite can absorb many negative ions, and moreover, the AuPdNPs can act as electronic relay systems to transfer electrons donated by BH_4^- to the nitro groups of 4-NP, which expected to lower the kinetic barrier and thus catalyse the reduction. As shown in Fig. S6, after addition of $NaBH_4$ into 4-NP solution, the colour quickly changed from light yellow to yellow green, and in the UV-vis absorption measurement, a strong absorption peak shifted from 316 nm to 400 nm due to the formation of 4-nitrophenolate anions in alkaline conditions (Fig. 3A). The absorbance of this peak remained unchanged with time in the absence of metallic catalyst (Fig. 3B and C) but decreased quickly with a small amount of AuPdNPs/GNs. Fig. 3D displays the time-dependent UV-vis absorption spectra, which show that the absorption of 4-nitrophenolate anions at 400 nm decreases along with a concomitant increase of the 303 nm peak of 4-aminophenol. This result is in accord with Fig. S6, with the adding of AuPdNPs/GNs, the yellow colour of the 4-NP solution is completely bleached in 5 min, signalling the completion of the reaction.

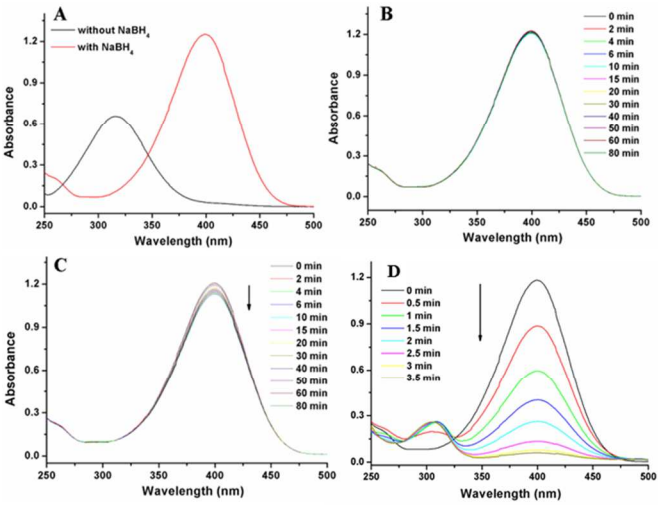

Fig. 3 UV-vis spectra of (A) 4-NP before and after addition of $NaBH_4$ solution, (B-D) Time-dependent UV-vis absorption spectra of reduction 4-NP by $NaBH_4$ (B) without any catalysts, in presence of (C) GNs and (D) AuPdNPs/GNs.

Esumi et al. has proposed that the catalytic reduction of 4-NP proceeded in two steps: (1) diffusion and adsorption of 4-NP to catalyst surface and (2) electron transfer mediated by the catalyst surface from BH_4^- to 4-NP.[34] Therefore, enhancing the adsorption ability and electron transfer property of the catalyst are both important for the reduction of 4-NP. To optimize the property of AuPdNPs/GNs and investigate the synergetic effects of Au and Pd in the 4-NP reduction, we studied the catalytic ability of monometallic AuNPs/GNs, PdNPs/GNs and bimetallic AuPdNPs/GNs with different atomic ratios of Au versus Pd. These experiments were carried out under the same conditions and the amount of each catalyst was controlled at 1.25 μg. As shown in Fig. 4, the morphology of the AuNPs and PdNPs are sphere, which are similar with AuPdNPs. Additionally, the average sizes of AuNPs and PdNPs are 3.15 and 2.67 nm, respectively, which is a little smaller than that of AuPdNPs. Based on these observations, the effects from morphology and size can be excluded when comparing the catalytic ability of mono- and bi- metallic NPs/GNs towards 4-NP reduction. From the time-dependent UV-vis absorption spectra, the time for PdNPs/GNs to complete the reaction is shorter than that for AuNPs/GNs, but it is much longer than that for AuPdNPs/GNs. This indicated that the catalytic activity of bimetallic AuPdNPs/GNs composites is highly enhanced over the monometallic AuNPs/GNs and PdNPs/GNs composite. Moreover, the optical properties and catalytic activities of the AuPdNPs/GNs composite are tunable via the Au versus Pd atomic ratios (V_m). As shown in Fig. S7, the reaction became rapidly with the increase of V_m value and reached the highest reaction rate on the $Au_{53}Pd_{47}$NPs/GNs catalyst.

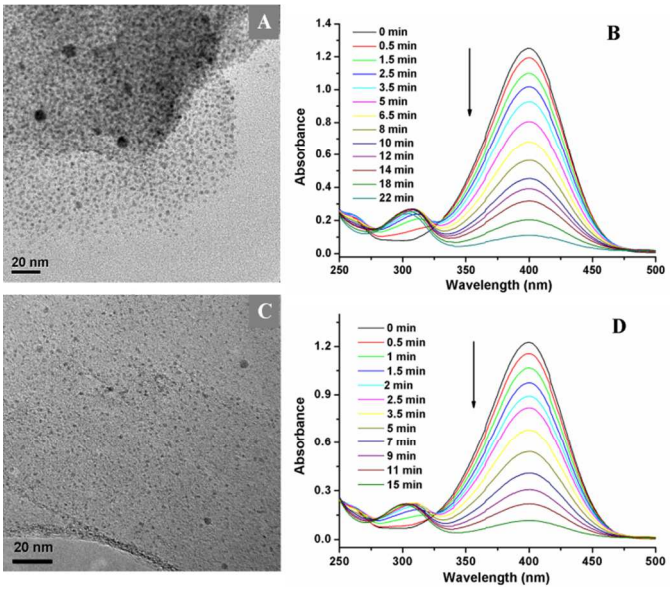

Fig. 4 TEM images of (A) AuNPs/GNs and (C) PdNPs/GNs and the time-dependent UV-vis absorption spectra of reduction 4-NP by $NaBH_4$ in the presence of (B) AuNPs/GNs and (D) PdNPs/GNs.

The amount of BH_4^- in the system is 100-times higher than that of 4-NP, which eliminates the influence of the donor BH_4^- on the catalytic reaction. This means that the reaction rate could be regarded to be independent of the BH_4^- concentration. Thus, pseudo-first-order kinetics were used to evaluate the rate of the catalytic reaction. The experiment was carried out under the same conditions for AuNPs/GNs (Fig. 4B), PdNPs/GNs (Fig. 4D) and several AuPdNPs/GNs catalysts (Fig. S7 and S8). As expected, linear relationships of ln (A_t/A_0) versus reaction time were obtained (Fig. 5), where A_t and A_0 represent the absorbance at the intervals and the initial stage of 4-nitrophenolate anions, respectively. It is clear that most AuPdNPs/GNs catalysts have a higher activity in compared with AuNPs/GNs and PdNPs/GNs, revealing the synergistic catalytic effect of Au and Pd species. Moreover, among all these catalysts, $Au_{53}Pd_{47}$NPs/GNs express the highest activity with a rate constant estimated to be 0.867 min^{-1}. As recognized from the change in the rate constants with the Au mole fraction (Fig. S8 and Table 1), the 1:1 mixing brought about the highest performance and the rate constant was faster than those reported Au- or Pd- based catalysts.[6-8, 10, 35-37]

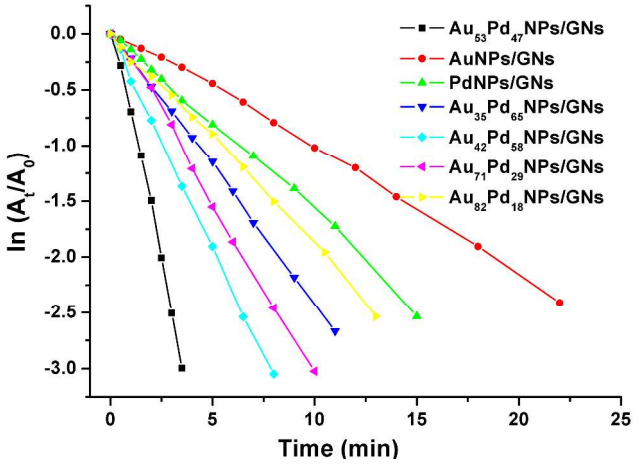

Fig. 5 Plot of $\ln(A_t/A_0)$ versus time for the reduction of 4-NP over different catalysts.

Table 1 Summary of the amounts of bimetallic precursors in the preparation approach, the weight percentage of Au and Pd (based on ICP-MS results), the molar ratios between Au and Pd, and the rate constants of the reaction (κ).

Sample	Preparation approach		Au (wt %)	Pd (wt %)	Au : Pd (molar)	κ (min^{-1})
	$HAuCl_4$ (mL)	K_2PdCl_4 (mL)				
1	0.5	0	25.7	-	-	0.109
2	0.5	0.125	22.3	2.6	82 : 18	0.190
3	0.5	0.25	24.0	5.3	71 : 29	0.313
4	0.5	0.5	25.2	12.1	53 : 47	0.867
5	0.5	0.75	23.6	17.5	42 : 58	0.385
6	0.5	1	25.5	25.4	35 : 65	0.244
7	0	0.5	-	16.0	-	0.164

The reusability of the AuPdNPs/GNs was also investigated. As shown in Fig. 6, the AuPdNPs/GNs can be reused four times without any significant loss of substrate conversion. In the fourth run, the rate constant for 4-NP reaction was still at 0.792 min^{-1}, which is about 91% as high as that of the first run. This result suggested that the as-prepared AuPdNPs/GNs exhibited a good reusability for the reduction of 4-NP.

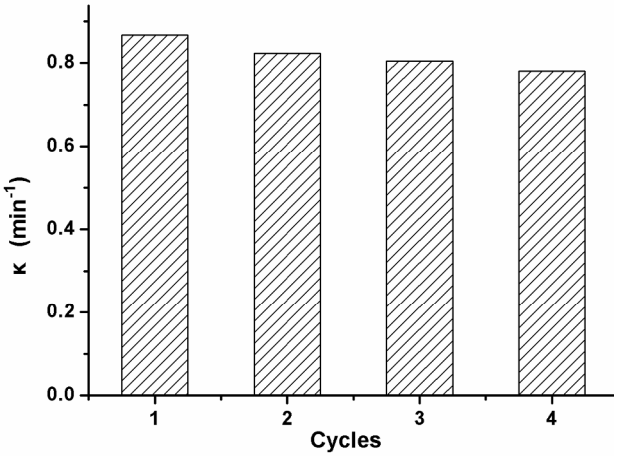

Fig. 6 Reusability of the $Au_{52}Pd_{48}$NPs/GNs as catalysts for the reduction of 4-NP by $NaBH_4$.

Conclusions

In summary, we have developed a facile and efficient route for synthesizing AuPdNPs on GNs with a very narrow size distribution by the redox reaction between bimetallic precursors and GNs. Due to the surfactant-free formation process, the prepared material is very clean, and usable as a high performance catalyst for the reduction of 4-NP. Moreover, the bimetallic AuPdNPs synergistically improve the catalytic activity compared to their monometallic NPs. The present findings might open up a new avenue in the development of high performance bimetallic NPs on proper supporting materials, which should be useful in heterogeneous catalysis.

Acknowledgements

Xiaomei Chen thanks the Japan Society for the Promotion of Science (JSPS) for the fellowship. This work was financially supported by the National Natural Science Foundation of China (No. 21305050), the Scientific Research Foundation of Shangda Li, Jimei Universtiy (ZC2013005), and JSPS KAKENHI Grant Nos. 24·02335 and 24550100.

Notes and references

[a]College of Biological Engineering, Jimei University, Xiamen, 361021, China. Email: xmchen@jmu.edu.cn
[b]State Key Laboratory of Marine Environmental Science and Department of Chemistry and the MOE Key Laboratory of Spectrochemical Analysis & Instrumentation, Xiamen University, Xiamen, 361005, China.
[c]Department of Material Chemistry, Graduate School of Engineering, Kyoto University, Nishikyo-ku, Kyoto, 615-8520, Japan

† Footnotes should appear here. These might include comments relevant to but not central to the matter under discussion, limited experimental and spectral data, and crystallographic data.

Electronic Supplementary Information (ESI) available: [TEM, XPS, XRD characterizations for AuPdNPs/GNs, details for the reduction of 4-NP.]. See DOI: 10.1039/b000000x/

1 X. Q. Huang, Y. J. Li, Y. Chen, H. L. Zhou, X. F. Duan and Y. Huang, *Angew. Chem. Int. Ed.*, 2013, **52**, 6063-6067.
2 L. F. Zhang, S. L. Zhong and A. W. Xu, *Angew. Chem. Int. Ed.*, 2013, **52**, 645-649.
3 Y. Sohn, D. Pradhan and K. T. Leung, *ACS Nano*, 2010, **4**, 5111-5120.
4 S. Zhang, Y. Y. Shao, H. G. Liao, J. Liu, I. A. Aksay, G. P. Yin and Y. H. Lin, *Chem. Mater.*, 2011, **23**, 1079-1081.
5 S. Zhang, Ö. Metin, D. Su and S. H. Sun, *Angew. Chem. Int. Ed.*, 2013, **52**, 3681-3684.
6 H. L. Jiang, T. Akita, T. Ishida, M. Haruta and Q. Xu, *J. Am. Chem. Soc.*, 2011, **133**, 1304-1306.
7 X. Zhang and Z. H. Su, *Adv. Mater.*, 2012, **24**, 4574-4577.
8 J. F. Huang, S. Vongehr, S. C. Tang, H. M. Lu and X. K. Meng, *J. Phys. Chem. C*, 2010, **114**, 15005-15010.
9 Q. An, M. Yu, Y. T. Zhang, W. F. Ma, J. Guo and C. C. Wang, *J. Phys. Chem. C*, 2012, **116**, 22432-22440.

10 J. W. Zhang, C. P. Hou, H. Huang, L. Zhang, Z. Y. Jiang, G. X. Chen, Y. Y. Jia, Q. Kuang, Z. X. Xie and L. S. Zheng, *Small*, 2013, **9**, 538-544.
11 F. Tao, M. E. Grass, Y. W. Zhang, D. R. Butcher, J. R. Renzas, Z. Liu, J. Y. Chung, B. S. Mun, M. Salmeron and G. A. Somorjai, *Science*, 2008, **322**, 932-934.
12 R. Ferrando, J. Jellinek and R. L. Johnston, *Chem. Rev.*, 2008, **108**, 845-910.
13 Y. Lu, J. Y. Yuan, F. Polzer, M. Drechsler and J. Preussner, *ACS Nano*, 2010, **4**, 7078-7086.
14 B. Chen, K. Lutker, S. V. Raju, J. Y. Yan, W. Kanitpanyacharoen, J. L. Lei, S. Z. Yang, H. -R. Wenk, H. Mao and Q. Williams, *Science*, 2012, **338**, 1448-1451.
15 J. A. Farmer and C. T. Campbell, *Science*, 2010, **329**, 933-936.
16 L. Zhao, C. Y. Zhang, L. Zhuo, Y. G. Zhang and J. Y. Ying, *J. Am. Chem. Soc.*, 2008, **130**, 12586-12587.
17 A. S. Barnard, *Acc. Chem. Res.*, 2012, **45**, 1688-1697.
18 C. Sivakumar and K. L. Phani, *Chem. Commun.*, 2011, **47**, 3535-3537.
19 O. M. Wilson, R. W. J. Scott, J. C. Garcia-Martinez and R. M. Crooks, *J. Am. Chem. Soc.*, 2005, **127**, 1015-1024.
20 A. Aijaz, A. Karkamkar, Y. J. Choi, N. Tsumori, E. Rönnebro, T. Autrey, H. Shioyama and Q. Xu, *J. Am. Chem. Soc.*, 2012, **134**, 13926-13929.
21 S. U. Son, Y. Jang, K. Y. Yoon, E. Kang and T. Hyeon, *Nano Lett.*, 2004, **4**, 1147-1151.
22 X. M. Chen, G. H. Wu, J. M. Chen, X. Chen, Z. X. Xie and X. R. Wang, *J. Am. Chem. Soc.*, 2011, **133**, 3693-3695.
23 S. Anandan, A. Manivel and M. Ashokkumar, *Fuel Cells*, 2012, **12**, 956-962.
24 W. Qian, R. Hao, J. Zhou, M. Eastman, B. A. Manhat, Q. Sun, A. M. Goforth and J. Jiao, *Carbon*, 2013, **52**, 595-604.
25 S. J. Guo and S. H. Sun, *J. Am. Chem. Soc.*, 2012, **134**, 2492-2495.
26 L. J. Cote, F. Kim and J. Huang, *J. Am. Chem. Soc.*, 2009, **131**, 1043-1049.
27 D. Li, M. B. Müller, S. Gilje, R. B. Kaner and G. G. Wallace, *Nat. Nanotechnol.*, 2008, **3**, 101-105.
28 H. J. Yin, H. J. Tang, D. Wang, Y. Gao and Z. Y. Tang, *ACS Nano*, 2012, **6**, 8288-8297.
29 H. Y. Koo, H. J. Lee, Y. Y. Noh, E. S. Lee, Y. H. Kim and W. S. Choi, *J. Mater. Chem.*, 2012, **22**, 7130-7135.
30 K. T. Chan, J. B. Neaton and M. L. Cohen, *Phys. Rev. B*, 2008, **77**, No. 235430.
31 P. A. Khomyakov, G. Giovannetti, P. C. Rusu, G. Brocks, J. Van den Brink and P. J. Kelly, *Phys. Rev. B*, 2009, **79**, No. 195425.
32 Y. W. Lee, M. Kim, Z. H. Kim and S. W. Han, *J. Am. Chem. Soc.*, 2009, **131**, 17036-17037.
33 M. M. Liu, Y. Z. Lu and W. Chen, *Adv. Funct. Mater.*, 2013, **23**, 1289-1296.
34 K. Hayakawa, T. Yoshimura and K. Esumi, *Langmuir*, 2003, **19**, 5517-5521.
35 Z. Jin, F. Wang, F. Wang, J. X. Wang, J. C. Yu and J. F. Wang, *Adv. Funct. Mater.*, 2013, **23**, 2137-2144.
36 K. Layek, M. L. Kantam, M. Shirai, D. Nishio-Hamane, T. Sasaki and H. Maheswaran, *Green Chem.*, 2012, **14**, 3164-3174.
37 H. Q. Li, L. N. Han, J. Cooper-White and I. Kim, *Green Chem.*, 2012, **14**, 586-591.